2023 IEEE International Conference on Robotics and Automation (ICRA 2023)
May 29 - June 2, 2023. London, UK

Dual quaternion based dynamic movement primitives to learn industrial tasks using teleoperation*

Rohit Chandra[1], Victor H. Giraud[1], Mohammad Alkhatib[1] , Youcef Mezouar[1]

Abstract— **Dynamic movement primitives (DMPs) provide an effective method of learning manipulation skills from human demonstration. DMPs can be especially useful for imitating industrial manipulation tasks which are performed by humans and are difficult to model, for instance, deformable object manipulation. In this work the effectiveness of a conventional Cartesian space DMP is enhanced using a compact and efficient representation of dual quaternions (DQ). We demonstrate that our DQ based DMP learning approach that utilizes the geometrical meaning of screw-based kinematics, outperforms traditional decoupled task-space DMPs in terms of accuracy during learning in certain situations. Our DMP formulation affords two additional applications: (1) Filter the noisy and irregular sensing of human demonstration; (2) Limit the robotic manipulator's task-space velocity during teleoperation, thus improving the safety of the robot and the environment. The learning and filtering strategies are validated on a bimanual robotic system and a motion capture system. We demonstrate the effectiveness of DMP based manipulation of deformable object by learning a bimanual deformation trajectory and then using it to perform the same task in new scenarios.**

I. INTRODUCTION

The study of robotic manipulation of deformable objects can be instrumental in relieving humans from tedious and repetitive tasks in industries dealing with production and handling of deformable objects for instance textiles, tires, *etc.* [1], [2]. However, there are several tasks still relying on human's manipulation skills. One of the main reasons for not using robots widely for those manipulation tasks has been the difficulty in task modeling [3]. The research community related to deformable object manipulation has focused on the modeling, sensing, and control aspects of the problem [4]–[6]. Few of the related work capitalize on the know-how of skillful workers. Some of notable few exceptions being, using Gaussian kernel model for origami folding task in [7], and using DMPs for cooperative transportation of deformable objects in [8], [9].

DMPs provide a framework to learn from demonstration. It can be used to realize movement planning of robots with the advantage of global stability and the possibility of incorporating feedback to modify the learned policies [10], [11].

*This work was done in the context of the SOFTMANBOT project, which received funding from the European Union's Horizon 2020 research and innovation programme under grant agreement number 869855. This work has also been funded by the European Union in the framework of the ERDF on the Ambition Research Pack initiated by the Auvergne Rhône Alpes Regional Council

[1]SIGMA, Université Clermont Auvergne, CNRS, Clermont Auvergne INP, Institut Pascal, F-63000 Clermont-Ferrand, France ol.alt.chandra@gmail.com, victor.giraud@sigma-clermont.fr, mohammad.alkhatib@sigma-clermont.fr, youcef.mezouar@sigma-clermont.fr.

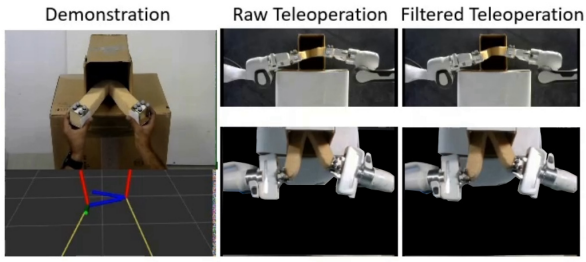

Fig. 1: *Foam in the box*: Final shape of the foam during human demonstration of the task and its imitation by a dual-arm Panda robot setup.

Since most of the approaches related to the manipulation of deformable objects consist of multi-agent systems, multiple DMPs related to these agents can be governed with one canonical system thus easing the problem of coordination [9]. Moreover, they can also help mitigate the following shortcomings related to many existing approaches related to deformation object manipulation:

- Many of these approaches use deformation Jacobians to compute the desired trajectory of robots for shape servoing. However, due to complexity of the deformation model and the inversion problem, numerical Jacobians are computed [4], [12], [13]. These deformation Jacobians work well around the vicinity of the current shape but they are subject to failure if large deformations are desired [14]. Learning from human demonstration can help "roughly" achieve the desired shape. Afterward, the existing deformation control approaches can be used for precise shape servoing by correcting the manipulators' trajectory to achieve the desired tasks during the operation.
- For the success of certain deformation tasks, it is important to respect certain spatial constraints in addition to precise shape control, for example transporting a deformable object while avoiding collision with obstacles [9]. Another example where active deformation is needed can be posing a filet on a pan. Although the starting and ending shapes are similar in this application, a particular trajectory is important to ensure maximum surface contact. A trajectory learned from human deformation can greatly simplify the problem of encoding these constraints and can allow the robots to execute a repetitive tasks faster.

In this work, we propose a novel task learning framework based on DMPs which uses the compact and efficient representation of unit dual quaternion (UDQ). The contributions

of our work can be summarised as follows:

- Our approach to DMP formulation using UDQ employs screw-based interpretation of rigid body transformation and exponential mapping of the screw parameters to get the corresponding UDQ. This ensures that the resulting dual quaternion always satisfies unity norm constraint. We also compare the performance of our "coupled" consideration of rotation and translation aspects of rigid body motion with conventional decoupled DMPs. We provide scenarios where our approach has a clear advantage over the decoupled approach.
- We apply the UDQ based DMP method for interpolating and filtering a Cartesian trajectory online, which can be used for safe teleoperation because our screw interpolation is capable of limiting the velocity twist to the desired value. The proposed interpolation and filtering approach can also be used to deal with irregular demonstration data tracking and corresponding noise. This preprocessing of the demonstration data also ensures better distribution of Gaussian radial basis functions (RBFs) along the phase associated with its DMP during policy learning.

In the next section (Sec. II) the related work in the domain of Cartesian space DMPs is reviewed with a focus on the aspect of their rigid body motion representation. The problem statement is outlined in Sec. III. The mathematical background necessary to understand the further mathematical developments has been presented in Sec. IV. We explain our approach for DQ based DMP in Sec. V and DMP based filtering strategy in Sec. VI, respectively. The experimental validation and a discussion on the results have been detailed in Sec. VII. Finally, conclusion and perspective of our work have been presented in Sec. VIII.

II. Related Work

Since the inception of DMP in [11], [15], there have been efforts to apply the method to learn the Cartesian trajectory of human demonstration [16], [17]. While the extension of the original single degree of freedom expression of DMP to learn position trajectories is trivial, the methodology to extend it to orientation trajectories has gained attention in the last few years.

Quaternions were used with DMP to learn the orientation component of human demonstration in [18]. They overcame the problem of non-unitary quaternions during motion generation, by learning only the vector components of the error quaternion instead of using all four components. The final quaternion was obtained by using quaternion propagation.

The quaternion based DMP for orientation proposed in [18] was employed for filtering the trajectory data online in [19]. Their filtering approach ensured bounded task-space angular velocity, thus making it safer for robot and the environment during learning of skills using teleoperation. They used SLERP to interpolate from between set-points related to orientation while respecting angular velocity limit. Their quaternion based DMP filter was also effective in dealing with jump discontinuity in the angular velocity. In this work, we deploy UDQ based DMP filter to limit the screw twist online during a teleoperation task.

Another approach for learning the control policies pertaining to orientation was given in [20] using rotation matrices. While logarithmic mapping of error rotation matrices was used for obtaining the orientation differences, exponential mapping was used to compute the final rotation matrix from the learned angular velocity. They also proposed a quaternion based approach where the logarithmic mapping was used to obtain error vector related to orientation, to preserve the geometric meaning of $SO(3)$. They noted that the quaternion based DMP were more stable due to the discontinuity in the logarithmic mapping of rotation matrices. In [21], Lyapunov based methods were used to prove the stability of the orientation DMP system with vector components ([18]) and logarithmic mapping of quaternion ([20]).

Dual quaternion based DMP system was used for learning Unmanned Aerial Vehicle's trajectories during acrobatic flight in [22]. They employed logarithmic mapping of error UDQ to get screw displacement parameters from rigid transformation. However, there is an inherent error in their UDQ based DMP formulation because of the incorrect computation of the dual component of the screw twist. They considered the actual translation vector between two poses as the dual part while referring to the work of [23] which in turn refers to [24] for its proof. The issue with the proof given in [23] is that they used the expression intended for dual numbers to deal with dual quaternions, which is wrong because of non-commutation in quaternion multiplications. For this reason their DMP system under-performs compared to the traditional decoupled DMP approach that learns position and quaternions part of movement separately.

An approach to derive task constraints from human demonstration and its application for new situations using screw motion and its representation using dual quaternions was given in [25]. In this work, we propose a more general framework for skill transfer from human to manipulators. We use dual quaterion based DMP filter for online filtering and learning of human demonstration trajectories using the same geometrically meaningful definition of motion.

III. Problem statement

Consider a sensing system capable of tracking the Cartesian pose of a robotic manipulator or human wrist at a frequency of f_h, where the pose being tracked is represented with a UDQ. We desire to generate higher frequency set-points for a robotic system following the trajectory during teleoperation, say f_m, with the following features:

- the velocity twist should be continuous
- the velocity twist should be lower than a pre-defined threshold ($\hat{\boldsymbol{\omega}}_{max} \in \mathbb{R}^6$) throughout the duration of teleoperation.

Now consider a demonstration of a task carried on by humans, either directly or by kinesthetically teaching a robotic system. We want to formulate a DMP based strategy for learning these tasks using dual quaternions representation, while relying on screw-based kinematics.

TABLE I: Mathematical notation.

Mathematical entity	Notation
Scalar numbers	Italics: $a,b,c \in \mathbb{R}$
Quaternions and vectors	Bold italics: $\boldsymbol{q},\boldsymbol{q}_r \in \mathbb{H}$
Dual numbers	Hat, italics: $\hat{a},\hat{b},\hat{c} \in \mathbb{DR}$
Dual quaternions and dual vectors	Hat, bold italics: $\hat{\boldsymbol{q}} \in \mathbb{DH}$

IV. Dual Quaternion

In this section we present some mathematical background to dual quaternions, the involved mathematical operations, screw based kinematics. For more details we refer the readers to [26] and [27]. We have used the mathematical symbols as described in Table I.

A. Screw displacement

The transformation between two poses can be expressed through screw displacement based on Chasles' theorem, which we depict in Fig. 2. The screw displacement is composed of four parameters: $\theta, \boldsymbol{\ell}, d$, and $\boldsymbol{m}$. An axis-angle rotation is represented by a rotation $\theta \in \mathbb{R}^+$ along an axis $\boldsymbol{\ell} \in \mathbb{R}^3$, while $d \in \mathbb{R}$ symbolizes a displacement over the same axis. Here $\boldsymbol{m} \in \mathbb{R}^3$ is a moment vector such that $\boldsymbol{m} \perp \boldsymbol{\ell}$.

We use a dual number. which we refer to as a dual angle to combine the rotation and translation parameters, $\hat{\theta} = \theta + \varepsilon d$. A directed or Plücker line is given as a dual vector $\hat{\boldsymbol{s}} = \boldsymbol{l} + \varepsilon \boldsymbol{m}$ (ε is a *dual unit*, such that $\varepsilon^2 = 0$). A screw displacement ($\hat{\boldsymbol{\vartheta}}$) can be represented as a dual vector:

$$\hat{\boldsymbol{\vartheta}} = \hat{\theta}\,\hat{\boldsymbol{s}} = \theta\boldsymbol{\ell} + \varepsilon(d\boldsymbol{\ell} + \theta\boldsymbol{m}), \tag{1}$$

Here $\boldsymbol{l}$ is the unit vector along the axis related to the screw displacement and $\boldsymbol{m} = \boldsymbol{p} \times \boldsymbol{l}$ corresponds to the moment of the directed line (Plücker line). $\boldsymbol{p}$ is a vector from the origin of a given reference frame to any point lying on the directed line (see Fig. 2).

B. Dual Quaternions

Dual quaternions are extension of dual numbers with quaternions as primary ($\boldsymbol{q}_r$) and dual ($\boldsymbol{q}_d$) components, and can be written in following forms:

$$\hat{\boldsymbol{x}} = \boldsymbol{q}_r + \varepsilon \boldsymbol{q}_d \tag{2}$$

C. Unit dual quaternions and screw displacements

A UDQ representing a pose defined based on a screw displacement, similar to the one shown in Fig. 2, can then be computed using exponential mapping as follows:

$$\begin{aligned}\hat{\boldsymbol{x}} = e^{\hat{\boldsymbol{\vartheta}}/2} &= \cos\left(\frac{\theta}{2}\right) + \boldsymbol{\ell}\sin\left(\frac{\theta}{2}\right) \\ &+ \varepsilon\left(-\frac{d}{2}\sin\left(\frac{\theta}{2}\right) + \boldsymbol{\ell}\,\frac{d}{2}\cos\left(\frac{\theta}{2}\right) + \boldsymbol{m}\sin\left(\frac{\theta}{2}\right)\right)\end{aligned} \tag{3}$$

Conversely, to derive screw parameters from a unit dual quaternions, we refer the readers to the logarithmic mapping approach given in [27].

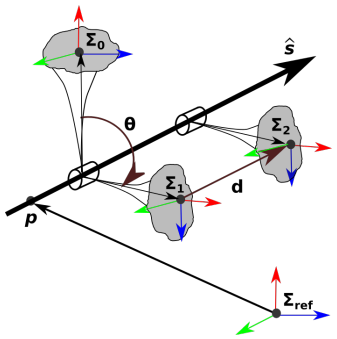

Fig. 2: Screw motion with a translation d, and a rotation θ over an axis $\vec{\ell}$, with a moment $\vec{m}$.

Classical dual quaternion conjugate of UDQ $\hat{\boldsymbol{x}}$ is used to invert the transformation and is defined as:

$$\hat{\boldsymbol{x}}^* = \boldsymbol{q}_r^* + \varepsilon \boldsymbol{q}_d^* \tag{4}$$

where $\boldsymbol{q}^*$ is the conjugate of quaternion $\boldsymbol{q}$.

V. Dual quaternion based DMPs

The formulation of a single degree of freedom DMP capable of temporal and spatial scaling is given as a second-order dynamical system, similar to a mass-spring-damper system [16]:

$$\tau\dot{y} = \mathbf{K}(g - x) - \mathbf{D}y - \mathbf{K}(g - x_0)s + \mathbf{K}f(s) \tag{5}$$

$$\tau\dot{x} = y \tag{6}$$

where x and x_0 is the current and the initial state of the system and g is the final position of the state. $\mathbf{K}$ and $\mathbf{D}$ are the stiffness and damping terms of point attractor dynamics. The system can be made critically damped by choosing the damping coefficient $\mathbf{D} = \sqrt{4\mathbf{K}\tau}$. The temporal scaling factor denoted with τ is used to speed-up or slow down the movement. The forcing term based on the phase is given by $f(s)$. The dynamics of the phase variable s is defined as:

$$\dot{s} = -\alpha_s s \tag{7}$$

where α_s refers to the time constant defining the rate of decay of the phase variable with time. The forcing function $f(s)$ is defined as:

$$f(s) = \frac{\sum_{i=1}^{N} \psi_i(s)\,\theta_i\,s}{\sum_{i=1}^{N} \psi_i(s)} \tag{8}$$

$$\psi_i(s) = e^{(-h_i(s-c_i)^2)} \tag{9}$$

Here Gaussian basis functions are denoted with $\psi_i(s)$ for $i = 1$ to N, defined using phase value $s(t)$, widths (h_i), and appropriately distributed centres (c_i). θ_i refers to the weight of the basis functions which are estimated while learning a movement primitive.

We modify the DMP formulation (5) to a 6-*dof* DMP driven by the same canonical system (7) to learn the screw twist derived from UDQ based representation of pose:

$$\tau\dot{\hat{\boldsymbol{\omega}}} = \mathbf{K}\hat{\boldsymbol{\vartheta}} - \mathbf{D}\hat{\boldsymbol{\omega}} - \mathbf{K}\hat{\boldsymbol{\vartheta}}_0 s + \mathbf{K}\mathbf{f}(s) \tag{10}$$

$$\tau\dot{\hat{\boldsymbol{\vartheta}}} = \hat{\boldsymbol{\omega}} \tag{11}$$

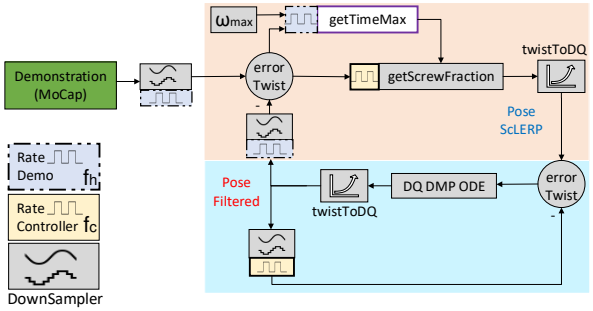

Fig. 3: Online trajectory filtering and learning: The top part of the block diagram corresponds to the filtering strategy while the bottom half deals with learning using DMP.

The screw distance $\hat{\boldsymbol{\vartheta}}$ between goal configuration ($\hat{\boldsymbol{x}}_g$) and current configuration ($\hat{\boldsymbol{x}}_t$) is computed as:

$$\hat{\boldsymbol{\vartheta}} = \ln(\hat{\boldsymbol{x}}_{(g-t)}) = \ln(\hat{\boldsymbol{x}}_t^* \hat{\boldsymbol{x}}_g) \tag{12}$$

We compute $\hat{\boldsymbol{\vartheta}}_0$ using the same approach and by replacing $\hat{\boldsymbol{x}}_t$ with the initial pose $\hat{\boldsymbol{x}}_0$. The twist velocity and acceleration, $\hat{\boldsymbol{\omega}}$ and $\dot{\hat{\boldsymbol{\omega}}}$ respectively, are computed by taking the time derivative of the screw distance computed from $\hat{\boldsymbol{x}}_{(g-t)}$.

VI. Smooth Trajectory Generation

In this section we describe our approach for interpolating between the poses received from a tracking system and filtering it with DQ based DMP presented in Fig. 3. The DQ based DMP filter can be used to derive set-points for a robotic manipulator pose controller working at a higher frequency.

Using *errorTwist* block, we first compute the total screw distance ($\hat{\boldsymbol{\vartheta}}_t$) between the actual pose of the manipulator ($\hat{\boldsymbol{x}}_{t_i}$) and the new pose $\hat{\boldsymbol{x}}_d$ received from the motion tracking system at sampling time t_i. We then compute the interpolation duration (T_m) for the given maximum velocity twist ($\hat{\boldsymbol{\omega}}_{max}$) desired for motion of the end-effector in *getTimeMax* block:

$$\hat{\boldsymbol{\vartheta}}_{t_i} = \ln(\Delta\hat{\boldsymbol{x}}_{t_i})/\Delta t = \ln(\hat{\boldsymbol{x}}_{t_i}^* \hat{\boldsymbol{x}}_d)/\Delta t \tag{13}$$

$$T_m = max(vec(\hat{\boldsymbol{\vartheta}}_{t_i})./vec(\hat{\boldsymbol{\omega}}_{max})) \tag{14}$$

where $./$ refers to element wise division of the vector components obtained by considering the dual vectors as arrays. We have to ensure that the manipulator does not move faster than the tracking signal arriving at f_h frequency. So we compute the allowed time T_q for the robotic controller as follows:

$$T_q = max(T_m, \frac{1}{f_h}). \tag{15}$$

We apply ScLERP to generate a smooth screw path between the poses. ScLERP is an interpolation approach for rigid transformations [28]. The intermediate poses $\hat{\boldsymbol{x}}_t$ for the robotic controller is computed in *getScrewFraction* block:

$$\hat{\boldsymbol{x}}_t = \hat{\boldsymbol{x}}_{t_i} (\hat{\boldsymbol{x}}_{t_i}^* \hat{\boldsymbol{x}}_d)^u = \hat{\boldsymbol{x}}_c e^{(u\hat{\boldsymbol{\vartheta}}_{t_i})/2}, \tag{16}$$

Every time a new pose is received, the interpolation parameter $u = (t - t_i)/T_q$ is reset to zero and screw distance $\hat{\boldsymbol{\vartheta}}_{t_i}$ in (13) is recomputed.

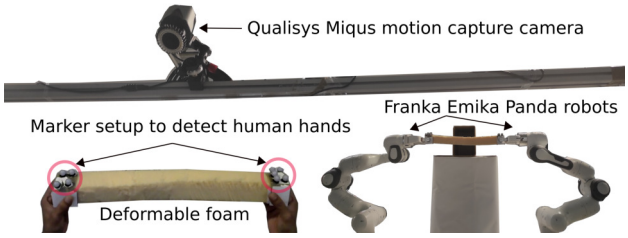

Fig. 4: Teleoperation setup consisting of Qualisys motion capture system, deformable foams with markers to record human demonstration trajectory and a dual-arm setup with Franka-Emika Panda robots.

For the purpose of filtering we ignore the forcing term $f(s)$ in (10). We first compute the screw displacement $\hat{\boldsymbol{\vartheta}}$ using (12). For that, we consider the ScLERP pose computed for the next time step $\hat{\boldsymbol{x}}_{t+\Delta t}$ in (16) as the goal configuration. We solve the differential equation (10) to obtain $\hat{\boldsymbol{\omega}}$ in *DQ DMP ODE* block. The velocity twist $\hat{\boldsymbol{\omega}}$ is integrated with controller rate f_c to obtain the new screw displacement for the filtered trajectory. The *twistToDQ* block then computes a corresponding UDQ displacement representing filtered pose using (3).

VII. Experimental Validation

We explain the strategy to validate our UDQ based approach for online trajectory filtering and learning of manipulation tasks using DMP in this section. In addition to demonstrating the effectiveness of our strategy, we highlight the difference between our coupled approach using screw-based kinematics and conventional decoupled approach. The complete robotic setup is shown in Fig. 4 which consisted of two Franka Emika Panda robots equipped with Franka Emika grippers and Qualisys motion capture system. We used ROS to interact with the robots and to collect data from human demonstration. The computer used for this validation had Intel Core i7-9850H CPU with 12 cores running at 2.60GHz.

In the next section (Sec. VII-A) the validation of filtering strategy is presented. Afterwards the experiments related to

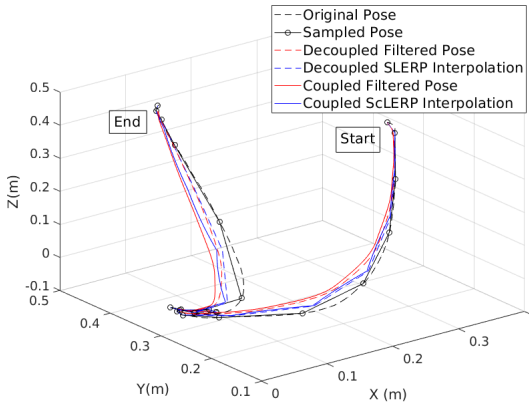

Fig. 5: Interpolation and filtering of pick and place task trajectory from human demonstration: Results for interpolation and filtering using decoupled approach is shown with dotted lines (blue and red, respectively), whereas the results related to the coupled strategy is represented with solid lines.

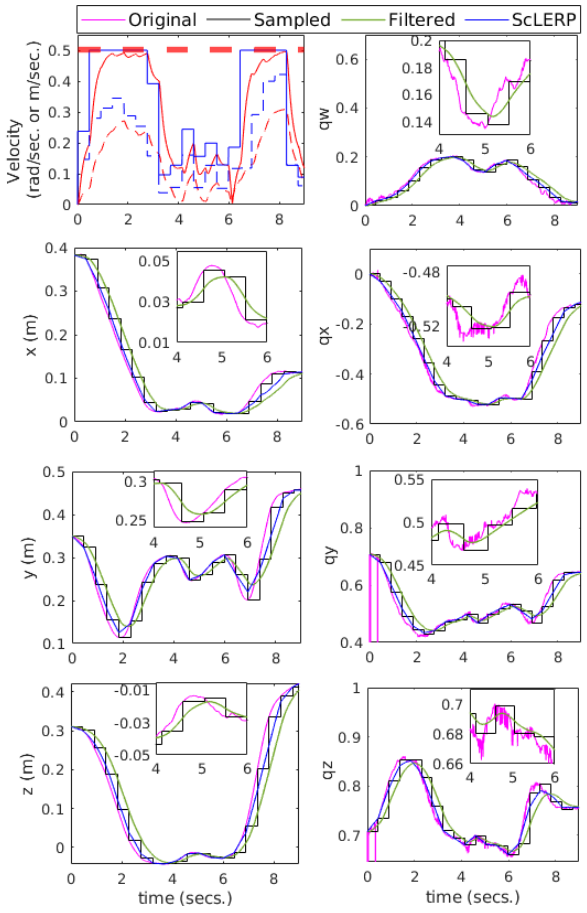

Fig. 6: Top left: Magnitude of the angular (solid lines) and linear velocity (dotted lines) of the generated trajectory: using only ScLERP over the sampled signal (shown in blue); and, using DMP filter with ScLERP (shown in red). The desired velocity limit is shown in thick dotted horizontal red line. Other plots depicts position and quaternion components of the original, sampled, interpolated and filtered pose. The zoomed plots only show the original, sampled and filtered plots for clarity.

learning manipulation task using DQ based DMP are detailed in Sec. VII-B.

A. Validation of Filtering Strategy

We recorded the trajectory of a human demonstration of pick and place task using the motion capture system from Qualisys motion capture system [29] shown in Fig. 4. The pose of the markers attached to the wrist of the demonstrator was received at $\approx 140\,Hz$. The original trajectory is shown in black dotted line in Fig. 5. We down-sampled the original signal to $2\,Hz$ which is represented with a solid black line. The goal of down-sampling the original signal to such a low frequency is to highlight the difference between coupled and decoupled approaches with regards to interpolation and filtering. The stiffness constant for the DMP based filter was chosen as $\mathbf{K} = 50$. The damping constant was computed for a critical damping response, and the time constant was set to $\tau = 1$.

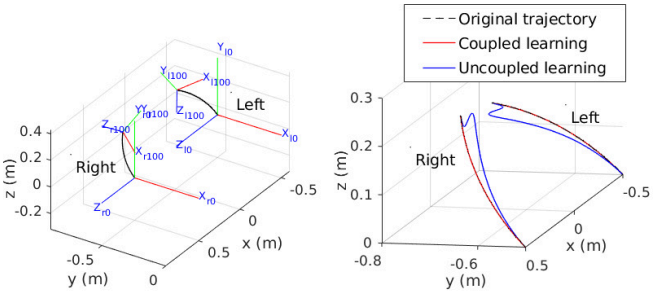

Fig. 7: Relative rotation task trajectory: The left figure shows the generated artificial trajectory involving relative rotation between two arms. The figure on the right side depicts the learnt trajectory. The learnt trajectory using our coupled approach is almost perfectly aligned with the original trajectory, while the one corresponding to decoupled approach has a significant deviation.

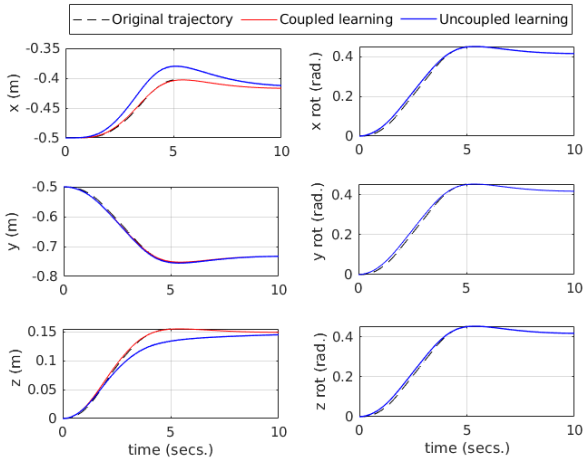

Fig. 8: Relative rotation task trajectory learning for left hand: Orientation components are represented with angle-axis components. Coupled trajectory is almost coincident with the original trajectory

The ScLERP interpolation for both coupled and decoupled approaches and corresponding filtered trajectories are also depicted in Fig. 5. It is evident that the ScLERP generated trajectories is a connected set of circular or screw arcs. SLERP and position based interpolation produced trajectory with straight lines in 3D space. The filtered trajectories, for both coupled and decoupled approach are bounded by their corresponding interpolated trajectories. In the case of higher stiffness gains during filtering, which is not shown here, the filtered trajectories for both filtering approaches move nearer to the their corresponding interpolated trajectories.

The velocity and pose plot for the trajectory hence generated is shown in Fig. 6. As it can be seen in the top-left plot of Fig. 6, both ScLERP and filter with ScLERP were able to limit the velocity twist to the desired limit of 0.5 m/sec and 0.5 $radian/sec$. While the velocity generated by ScLERP interpolation was constant for the duration of the sampling, it had step jump discontinuity whenever a new pose was received from sampling. The trajectory generation strategy using both DMP based filter and ScLERP based interpolation

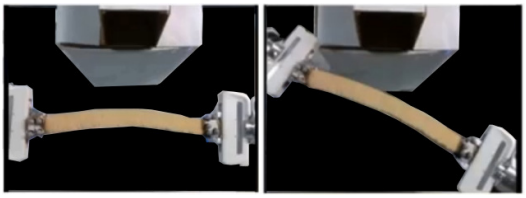

Fig. 9: Initial configuration during teleoperation (left), and during DMP execution after learning (right).

was successful in generating continuous velocity for both linear and rotational components.

B. Validation of DMP based learning strategy

We designed two experiments for the validation of our proposed DQ based DMP. In the first experiment we generated a synthetic trajectory to compare our approach with the conventional decoupled approach. Additionally, we learnt and executed a bimanual deformation task with trajectories obtained from human demonstration. Both of the tasks are detailed in the following subsections.

1) Synthetic trajectory from relative rotation: After observing the differences between coupled and decoupled approaches of interpolation and filtering (see Fig. 5) we designed an experiment to see if this difference translates to learning trajectories using DMPs as well. We considered a dual-arm robotic system and imposed a relative rotation between them along an arbitrary axis, similar to two arms operating a pair of scissors, while keeping the location of the hinge of the scissors constant. The trajectory was generated with a parabolic trajectory parameterized by translation $d = 0$ and rotation $\theta = 0\, to\, \pi/2$ (see (3)), over a duration of 5 *secs*.

The trajectory hence generated and the path taken by the coupled and decoupled DMP learning methods can be seen in Fig. 7. The position and orientation component of the original, and the trajectories learnt using both the approaches are given in Fig. 8. We use the same value of the parameters $\mathbf{K}$ and $\mathbf{D}$ for all the 6 components of the trajectory. We tuned them for the best performance of the decoupled approach and then used the same gain for our approach. It is clear from Fig. 8 that the x and z components need different stiffness gains to learn the trajectory more accurately in the case of decoupled approach. On the other hand, the coupled approach does not require tuning for individual components and can learn trajectory more accurately, as it can be seen in Fig. 7 and 8.

2) Bimanual deformation task: We also validated our approach with real robots with a deformation task which demonstrated the effectiveness of DMP for such tasks.

We performed a demonstration of deforming a linear foam in a certain shape to be able to fit it in a smaller box, as shown in Fig. 1. We recorded trajectories of the end points of the foam by tracking the markers fixed on the ends of the foam with Qualisys Tracking Manager. While the position tracking was fairly reliable, we noticed that the orientation part of the received trajectories were noisy. The trajectories received from the motion capture system were fed at 50 Hz to the DMP filter and the filtered trajectory was recorded at the same frequency. In order to mitigate the effects of noisy

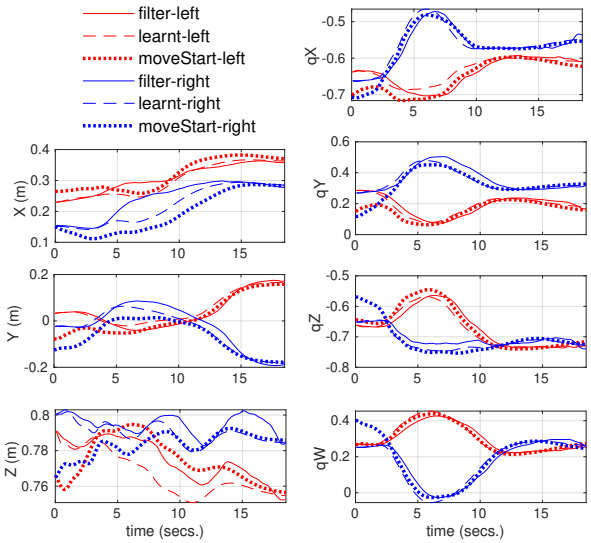

Fig. 10: Filtered input demostration, learnt and new starting pose trajectories for left (red) and right (blue) arms.

tracking of markers, we used the filtered trajectories for DMP based learning. We chose $\mathbf{K} = 25$ and $\alpha_s = 0.1$ using trial and error approach.

In order to highlight the effectiveness of learning based approach for the manipulation of deformable objects, we changed the starting configuration of the robotic arms, while maintaining the relative pose, as depicted in Fig. 9. Fig. 10 plots the input filter, learnt and adapted trajectories to new starting poses, named as *moveStart-*{*left*, *right*} during online execution with a real dual-arm Franka-Emika Panda robot setup. We confirm that the robot was able to successfully complete the *Foam in a box* task and final shape of the foam was very close to that of the learnt DMP [1].

VIII. CONCLUSIONS

We proposed a novel strategy for learning from human demonstration with a UDQ based DMP formulation. We used UDQ representation of poses and screw-based kinematic to formulate coupled DMP for learning Cartesian pose trajectories. We demonstrated that our approach performs better in comparison to traditional decoupled DMPs that learned position and orientation separately for tasks where coupled movement is desired. We validated our approach with a bimanual foam deformation task and demonstrated the effectiveness of our strategy of handling new situation. We also validated our filtering strategy based on DQ-DMP with a demonstration data for a pick and place task. We were also able to limit the velocity twist to a desired value. Our online filtering approach can be useful for making teleoperation safer.

In the future we would like to add feedback to the deformation control approach. We plan to use visual sensor to record the current shape during the demonstration and use them to correct the motion of the robot, thus closing the shape control loop.

[1] Video link: https://tinyurl.com/2p9arxre

REFERENCES

[1] J. Swanepoel, "The relationship between occupational risk and labour relations in a tyre manufacturing company," Ph.D. dissertation, 2014.

[2] D. Metgud, S. Khatri, M. Mokashi, and P. Saha, "An ergonomic study of women workers in a woolen textile factory for identification of health-related problems," *Indian journal of occupational and environmental medicine*, vol. 12, no. 1, p. 14, 2008.

[3] J. Sanchez, J.-A. Corrales, B.-C. Bouzgarrou, and Y. Mezouar, "Robotic manipulation and sensing of deformable objects in domestic and industrial applications: a survey," *The International Journal of Robotics Research*, p. 0278364918779698, 2018.

[4] M. Aranda, J. A. C. Ramon, Y. Mezouar, A. Bartoli, and E. Özgür, "Monocular visual shape tracking and servoing for isometrically deforming objects," in *2020 IEEE/RSJ International Conference on Intelligent Robots and Systems (IROS)*. IEEE, 2020, pp. 7542–7549.

[5] M. Beetz, U. Klank, A. Maldonado, D. Pangercic, and T. Rühr, "Robotic roommates making pancakes - look into perception-manipulation loop," in *IEEE International Conference on Robotics and Automation (ICRA), Workshop on Mobile Manipulation: Integrating Perception and Manipulation*, May, 9–13 2011, pp. 529–536.

[6] M. Takizawa, S. Kudoh, and T. Suehiro, "Method for placing a rope in a target shape and its application to a clove hitch," in *Robot and Human Interactive Communication (RO-MAN), 2015 24th IEEE International Symposium on*. IEEE, 2015, pp. 646–651.

[7] A. Namiki and S. Yokosawa, "Origami folding by multifingered hands with motion primitives," *Cyborg and Bionic Systems*, vol. 2021, 2021.

[8] D. Huang, B. Li, Y. Li, and C. Yang, "Cooperative manipulation of deformable objects by single-leader-dual-follower teleoperation," *IEEE Transactions on Industrial Electronics*, 2022.

[9] Z. Cui, W. Ma, J. Lai, H. K. Chu, and Y. Guo, "Coupled multiple dynamic movement primitives generalization for deformable object manipulation," *IEEE Robotics and Automation Letters*, vol. 7, no. 2, pp. 5381–5388, 2022.

[10] W. Si, N. Wang, and C. Yang, "A review on manipulation skill acquisition through teleoperation-based learning from demonstration," *Cognitive Computation and Systems*, vol. 3, no. 1, pp. 1–16, 2021.

[11] S. Schaal, "Dynamic movement primitives-a framework for motor control in humans and humanoid robotics," in *Adaptive motion of animals and machines*. Springer, 2006, pp. 261–280.

[12] D. Navarro-Alarcón, Y.-H. Liu, J. G. Romero, and P. Li, "Model-free visually servoed deformation control of elastic objects by robot manipulators," *IEEE Transactions on Robotics*, vol. 29, no. 6, pp. 1457–1468, 2013.

[13] M. Shetab-Bushehri, M. Aranda, Y. Mezouar, and E. Ozgur, "As-rigid-as-possible shape servoing," *IEEE Robotics and Automation Letters*, 2022.

[14] J. Zhu, B. Navarro, P. Fraisse, A. Crosnier, and A. Cherubini, "Dual-arm robotic manipulation of flexible cables," in *2018 IEEE/RSJ International Conference on Intelligent Robots and Systems (IROS)*. IEEE, 2018, pp. 479–484.

[15] A. J. Ijspeert, J. Nakanishi, and S. Schaal, "Movement imitation with nonlinear dynamical systems in humanoid robots," in *Proceedings 2002 IEEE International Conference on Robotics and Automation (Cat. No. 02CH37292)*, vol. 2. IEEE, 2002, pp. 1398–1403.

[16] P. Pastor, H. Hoffmann, T. Asfour, and S. Schaal, "Learning and generalization of motor skills by learning from demonstration," in *2009 IEEE International Conference on Robotics and Automation*. IEEE, 2009, pp. 763–768.

[17] A. Gams, M. Do, A. Ude, T. Asfour, and R. Dillmann, "On-line periodic movement and force-profile learning for adaptation to new surfaces," in *2010 10th IEEE-RAS International Conference on Humanoid Robots*. IEEE, 2010, pp. 560–565.

[18] P. Pastor, L. Righetti, M. Kalakrishnan, and S. Schaal, "Online movement adaptation based on previous sensor experiences," in *2011 IEEE/RSJ International Conference on Intelligent Robots and Systems*. IEEE, 2011, pp. 365–371.

[19] R. Weitschat, A. Dietrich, and J. Vogel, "Online motion generation for mirroring human arm motion," in *2016 IEEE International Conference on Robotics and Automation (ICRA)*. IEEE, 2016, pp. 4245–4250.

[20] A. Ude, B. Nemec, T. Petrić, and J. Morimoto, "Orientation in cartesian space dynamic movement primitives," in *2014 IEEE International Conference on Robotics and Automation (ICRA)*. IEEE, 2014, pp. 2997–3004.

[21] M. Saveriano, F. Franzel, and D. Lee, "Merging position and orientation motion primitives," in *2019 International Conference on Robotics and Automation (ICRA)*. IEEE, 2019, pp. 7041–7047.

[22] R. Zhang, Y. Hu, K. Zhao, and S. Cao, "A novel dual quaternion based dynamic motion primitives for acrobatic flight," in *2021 5th International Conference on Robotics and Automation Sciences (ICRAS)*. IEEE, 2021, pp. 165–171.

[23] X. Wang, C. Yu, and Z. Lin, "A dual quaternion solution to attitude and position control for rigid-body coordination," *IEEE Transactions on Robotics*, vol. 28, no. 5, pp. 1162–1170, 2012.

[24] O. Bottema and B. Roth, *Theoretical kinematics*. Courier Corporation, 1990, vol. 24.

[25] D. Mahalingam and N. Chakraborty, "Human-guided planning for complex manipulation tasks using the screw geometry of motion," *arXiv preprint arXiv:2209.05672*, 2022.

[26] Clifford, "Preliminary sketch of biquaternions," *Proceedings of the London Mathematical Society*, vol. s1-4, no. 1, pp. 381–395, nov 1871. [Online]. Available: https://doi.org/10.1112/plms/s1-4.1.381

[27] E. Özgür and Y. Mezouar, "Kinematic modeling and control of a robot arm using unit dual quaternions," *Robotics and Autonomous Systems*, vol. 77, pp. 66–73, 2016.

[28] L. Kavan, S. Collins, C. O'Sullivan, and J. Zara, "Dual quaternions for rigid transformation blending," *Trinity College Dublin, Tech. Rep. TCD-CS-2006-46*, 2006.

[29] "Qualisys motion capture system," https://www.qualisys.com//, [Online; accessed 30-May-2022].